Journal of Sound and Vibration (1998) **216**(4), 673–696
Article No. sv981706

MODAL ANALYSIS IN LINED WEDGE-SHAPED DUCTS

F. P. MECHEL
D-71120 *Grafenau* 1, *Germany*

(*Received* 28 *July* 1997, *and in final form* 16 *April* 1998)

It has been suggested to describe the sound field in a wedge-shaped duct in a cylindrical co-ordinate system in which the boundaries of the wedge lie in a co-ordinate surface. This suggestion was developed in a companion paper [1]. The wave equation can be separated only if the boundaries are ideally reflecting (rigid or soft). Two solutions were proposed in reference [1] for absorbing boundaries. In the first solution, the sound field is composed of "ideal modes" (modes in a wedge with ideally reflecting boundaires); the boundary condition at the absorbing boundary then leads to a system of equations for the mode amplitudes. The problem with this method lies in the fact that there is no radial orthogonality of the ideal modes so that the precision of the field synthesis by ideal modes is doubtful. In the second method in reference [1] one defines "fictitious modes" which satisfy the boundary conditions at the flanks exactly and which are based on hypergeometric functions as radial functions, but which produce a "rest" in the wave equation. It was described how this rest can be minimized; this procedure leads to slow numerical integrations. In the present paper, the wedge is subdivided into duct sections with parallel walls (the boundary is stepped); the fields in the sections are composed of duct modes (modes in a straight lined duct); the mode amplitudes are determined from the boundary conditions at the section limits. The advantages of the present method are (analytically) the duct modes are orthogonal across the sections, so the mode amplitudes can be determined with the usual precision of a modal analysis, and (numerically) no numerical integrations are needed.

1. INTRODUCTION

The operation costs per year of big industrial silencers (electrical power consumed by the static pressure loss of the silencer) may exceed the costs of the investment in them. A possibility for the reduction of the static pressure loss is the application of silencer cascades: the silencer is subdivided into sections with free duct widths of the sections tuned to high attenuation in different frequency bands (examples of stepped silencer cascades are described in reference [2]). The advantage of the silencer cascading, however, is reduced if the transitions between the sections are stepped. Wedge-shaped lined transitions evidently would be advantageous. A further field of applications of wedge-shaped ducts are the broadening transitions between the duct and a splitter type silencer as well as the contracting transitions from the silencer section to the duct. Because such wedge-shaped duct sections (with lined or rigid flanks) will act as mode filters, it would be necessary for a good

0022–460X/98/390673 + 24 $30.00/0

silencer design to have a theory available which describes the sound field in the wedge for an arbitrary modal content of the exciting sound wave at the entrance of the wedge.

The analysis of the sound field in wedge-shaped ducts is simple if the wedge boundaries are ideally reflecting; the "ideal modes" in such sections separate into products of trigonometric functions for the azimuthal dependence and cylindrical functions (Bessel, Neumann, Hankel functions) for the radial dependence in a cylindrical co-ordinate system (r, ϑ) which contains the wedge boundaries as co-ordinate surfaces. The "ideal modes" are orthogonal over the wedge angle. So one can try to compose the sound field in a wedge-shaped duct with absorbing boundaries by a superposition of ideal modes. The boundary condition at the absorbing boundary will lead to a system of equations for the mode amplitudes (see reference [1]). Even when it is assumed that the ideal modes are a complete system for the description of general sound fields, there remains the principal problem that there do not exist orthogonality relations for the ideal modes along the flank so that the precision of numerical solutions for the mode amplitudes cannot be guaranteed. A second approach to a solution, therefore, was described in reference [1], in which "fictitious modes" are defined which exactly satisfy the boundary condition at the absorbing flank and are orthogonal over the wedge angle. These fictitious modes have the shape. $T(\eta(r)\vartheta)R(r)$ in which $T(\eta(r)\vartheta) = \cos(\eta(r)\vartheta)$ or $T(\eta(r)\vartheta) = \sin(\eta(r)\vartheta)$ for modes which are symmetrical with respect to $\vartheta = 0$ or antisymmetrical, respectively, and $R(r)$ are hypergeometric functions. The azimuthal wave number $\eta(r)$ is a function of r; it is one of the solutions of the characteristic equation (different solutions define different fictitious modes). The fictitious modes, however, produce a "rest" of the wave equation solution. Two methods are described in reference [1] of how the rest can be minimized. Both methods need numerical integrations which would make the application of fictitious modes in numerical computations rather slow.

A completely different method of construction of modes in a wedge-shaped space with an absorbing flank was described by Felsen, Arnold and Topuz in references [3, 4] for the important underwater acoustic application of an inclined absorbing seabed. The present author did not succeed in transforming their method from the condition of a soft upper boundary to a rigid upper boundary and from a bulk reacting lower boundary to a locally reacting lower boundary. The reasons for the failure were not these differences, but the "remainder function" $E(\theta)$ of those authors. This remainder was neglected by the authors under the condition that the wedge angle is small (smaller than 3°), a condition which does not hold in duct applications. In fact, the (transformed) function $E(\theta)$ diverges "super-exponentially" (exponential increase of the exponent in an exponential function) at the ends of the integration path C in the complex plane of θ in references [3, 4] and also at the ends of any other reasonable path of integration. Therefore, the method of Felsen, Arnold and Topuz could not be transformed for silencer duct applications.

Instead, a construction of wedge modes by "duct modes" shall be described below. The duct modes are modal solutions in a straight lined duct of (half) duct height h, lined with a locally reacting absorber having a normalized surface

admittance G. These duct modes are orthogonal to each other over the duct width. The wedge-shaped duct will be approximated (in the computation only) by a stepped cascade of straight duct sections. The sound field in a section is formulated as a superposition of the duct modes of that section. Due to the orthogonality of the duct modes, the boundary conditions at the end planes of the sections (fitting of the sound pressure and of the axial particle velocity) can be solved for the modal amplitudes with the precision of the usual modal analysis (which is a Fourier analysis over space and wave numbers and as such gives the fits of the sound fields with a minimum average squared error). The mode order of the field solution in the wedge is defined by the mode order of a single duct mode which is incident on the wedge from a straight entrance duct having the width of the entrance plane of the wedge and the same lining as the wedge. The task will be formulated for a given, arbitrary mode mix of the incident modes.

2. THE OBJECTS

We consider the converging stepped wedge as in Figure 1(a) and the diverging stepped wedge as in Figure 1(b). Only one half of the wedge is shown; the plane $y = 0$ is either a plane of symmetry of the sound field and of the duct or a plane of antisymmetry of the field.

The sections (including the entrance duct) are numbered with $i = 0, 1, \ldots, I$; $i = 0$ belongs to the entrance duct. All sections are lined with a locally reacting absorber having a normalized (by the characteristic impedance Z_0 of air) admittance G; their duct heights are h_i and the length Δx; the step height is Δy. The axial co-ordinate of the end of the ith section is x_i, its entrance is at x_{i-1} (except for the entrance duct which is assumed to be infinitely long, see for the role of x_{-1}). The wedge is assumed to be terminated by a normalized admittance G_t (for reasons of simplicity; for more general terminations see below). The wedge is excited by a set of modes incident from the entrance duct with the vector $\{A_{0,m}\}$ of mode amplitudes. The incident modes can either be symmetrical with respect to $y = 0$ or antisymmetrical. The fields in the wedge sections retain the type of symmetry. Skew fields with respect to $y = 0$ can be described by a superposition of symmetrical and antisymmetrical modes which do not couple with each other. A time factor $e^{j\omega t}$ is supposed for all field components. The free-field wave number is $k_0 = \omega/c_0$ (c_0 is the speed of sound).

The locally reacting absorber as the duct lining is chosen here for reasons of simplicity; the orthogonality relation of the duct modes then is simpler than with a bulk reacting absorber (for fields in a wedge with a bulk reacting absorber, see reference [2, chapter 4]).

3. FORMULATION OF THE SOUND FIELD

The field $p_i(x, y)$ is composed in the ith section by forward waves $p_{e,i}(x, y)$ and backward waves $p_{r,i}(x, y)$ which themselves are superpositions of duct modes:

$$p_{e,i}(x, y) = \sum_{m \geqslant 0} A_{i,m} q_{i,m}(y)\, e^{-\gamma_{i,m}(x - x_{i-1})}, \tag{1}$$

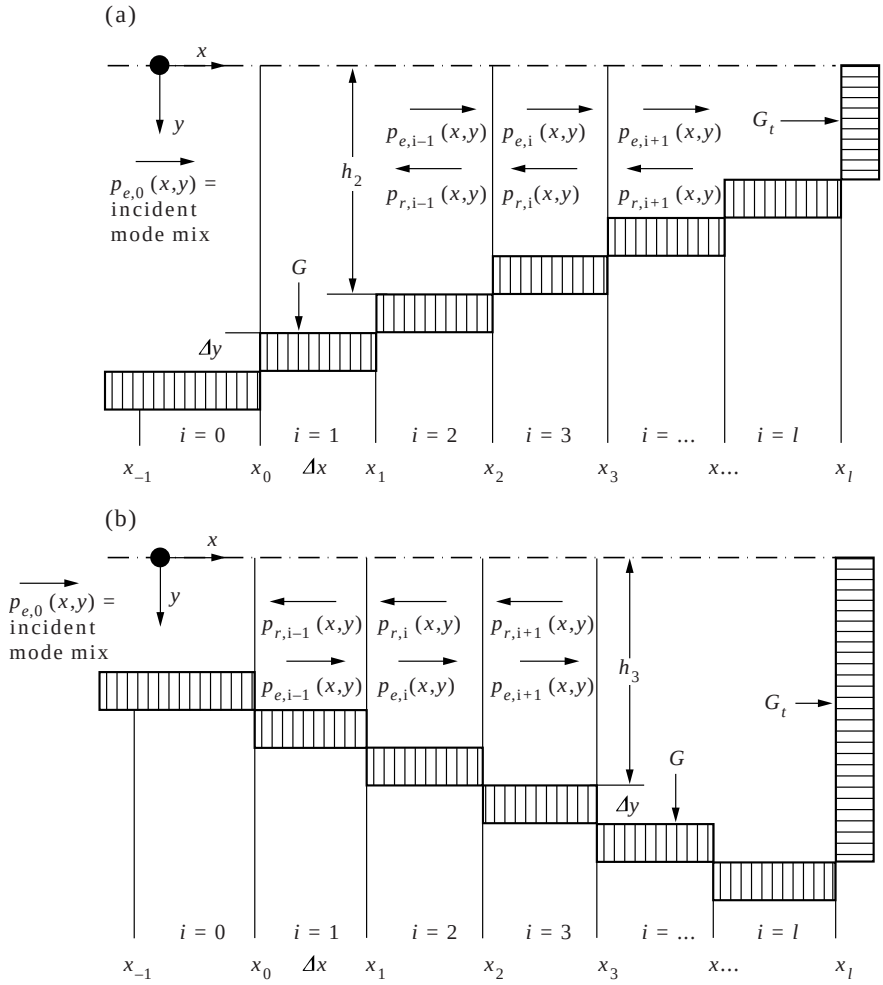

Figure 1. (a) A stepped converging wedge-shaped duct following a straight entrance duct, both lined with a locally reacting absorber of (normalized) admittance G. The wedge is terminated with a locally reacting absorber of (normalized) admittance G_t. The wedge sections are numbered $i = 1, 2, \ldots, l$; the entrance duct belongs to $i = 0$; the section height is h_i; the section length is Δx. (b) A stepped diverging wedge; otherwise as in Figure 1(a).

$$p_{r,i}(x, y) = \sum_{m \geqslant 0} B_{i,m} q_{i,m}(y)\, \mathrm{e}^{+\gamma_{i,m}(x - x_i)}. \tag{2}$$

The amplitudes $A_{i,m}$ of the forward modes are "defined" in the entrance plane $x = x_{i-1}$ of the ith section; the amplitudes $B_{i,m}$ of the backward modes are "defined" in the exit plane $x = x_i$; the amplitudes $A_{0,m}$ of the incident modes are defined at $x_{-1} = x_0 - \Delta x$ in order to retain the scheme. The lateral profiles of the duct modes are

$$q_{i,m}(y) = \begin{Bmatrix} \cos(\varepsilon_{i,m} y), & \text{symmetrical} \\ \sin(\varepsilon_{i,m} y), & \text{antisymmetrical} \end{Bmatrix}. \tag{3}$$

The wave equation delivers the relation between the lateral wave numbers $\varepsilon_{i,m}$ and the axial propagation constants $\gamma_{i,m}$ as

$$\gamma_{i,m}^2 = \varepsilon_{i,m}^2 - k_0^2, \qquad \mathrm{Re}\,\{\gamma_{i,m}\} \geqslant 0, \tag{4}$$

where the sign convention corresponds to the farfield condition. The boundary condition at the absorbing wall of the duct sections leads to the characteristic equations

$$\begin{aligned} (\varepsilon_{i,m}h_i)\tan(\varepsilon_{i,m}h_i) &= \mathrm{j}k_0 h_i G, \qquad \text{symmetrical.} \\ (\varepsilon_{i,m}h_i)\cot(\varepsilon_{i,m}h_i) &= -\mathrm{j}k_0 h_i G, \qquad \text{antisymmetrical.} \end{aligned} \tag{5}$$

A mode-safe (i.e., safe against jumping between modes) and fast algorithm for their solution for a set $m = 0, 1, 2, \ldots$ of modes in the sections $i = 0, 1, \ldots, , I$ is described in reference [1]. The exceptional role of the surface wave mode (a mode which decays exponentially away from the absorber) is also discussed there.

One will need the norms $N_{i,m}$ of the duct modes,

$$\frac{1}{h_i}\int_0^{h_i} q_{i,m}(y)q_{i,n}(y)\,\mathrm{d}y = \delta_{m,n}N_{i,m}, \qquad N_{i,m} = \frac{1}{2}\left(1 \pm \frac{\sin(2\varepsilon_{i,m}h_i)}{2\varepsilon_{i,m}h_i}\right), \tag{6}$$

and the coupling coefficients $C(i,m;k,n)$ of the mode of order m in the section i with the mode of order n in the section k:

$$\frac{1}{h_i}\int_0^{h_i} q_{i,m}(y)q_{k,n}(y)\,\mathrm{d}y = C(i,m;k,n),$$

$$C(i,m;k,n) = \frac{1}{2}\left(\frac{\sin(\varepsilon_{i,m}-\varepsilon_{k,n})h_i}{(\varepsilon_{i,m}-\varepsilon_{k,n})h_i} \pm \frac{\sin(\varepsilon_{i,m}+\varepsilon_{k,n})h_i}{(\varepsilon_{i,m}+\varepsilon_{k,n})h_i}\right). \tag{7}$$

The signs correspond to symmetrical and antisymmetrical modes, respectively. Note that with $k = i$ in equations (7), one has the integral of equation (6), and the orthogonality of the modes is shown by collecting the two fractions into one denominator and expanding the sin (. . .) of the difference and sum, then inserting equations (5) and taking into account that G does not depend on the mode order.

With our special termination of the wedge with an admittance G_t one has

$$\{B_{I,m}\} = \{M_t\} \circ \{A_{I,m}\} = \{r_m\,\mathrm{e}^{-\gamma_{I,m}\Delta x}\} \circ \{A_{I,m}\}, \tag{8}$$

where $\{M_t\}$ is a general coupling matrix ($\circ$ is the sign of matrix multiplication), which in this special case is a diagonal matrix with the values $r_m\,\mathrm{e}^{-\gamma_{I,m}\Delta x}$ on the main diagonal, where r_m are the modal reflection factors at the exit of the last section $i = I$,

$$r_m = \frac{g_m - G_t}{g_m + G_t} = \frac{\mathrm{j}\gamma_{I,m}/k_0 + G_t}{\mathrm{j}\gamma_{I,m}/k_0 - G_t}, \tag{9}$$

and g_m are the normalized axial modal admittances of the modes of $p_{e,I}(x, y)$,

$$g_m = Z_0 \frac{vx_{eI,m}(x_I)}{p_{eI,m}(x_I)} = -\mathrm{j}\frac{\gamma_{I,m}}{k_0}. \tag{10}$$

In other, more general cases of termination, e.g., by a lateral absorber or by a duct (lined or with rigid walls) which itself is properly terminated, it can be shown that the first form of equation (8) holds (with $\{M_t\}$ no longer diagonal). In principle it is that general form of equation (8) which will be applied below.

4. MODAL ANALYSIS IN THE CONVERGING WEDGE

The boundary condition for the sound pressure at the entrance $x = x_{i-1}$ of the ith section ($i \geqslant 1$) is ($\ldots \stackrel{!}{=} \ldots$ indicates a requirement)

$$p_{e,i-1}(x_{i-1}, y) + p_{r,i-1}(x_{i-1}, y) \stackrel{!}{=} p_{e,i}(x_{i-1}, y) + p_{r,i}(x_{i-1}, y), \qquad 0 \leqslant y \leqslant h_i, \tag{11a}$$

$$\sum_m (A_{i-1,m}\, \mathrm{e}^{-\gamma_{i-1,m}\Delta x} + B_{i-1,m}) q_{i-1,m}(y) \stackrel{!}{=} \sum_m (A_{i,m} + B_{i,m}\, \mathrm{e}^{-\gamma_{i,m}\Delta x}) q_{i,m}(y). \tag{11b}$$

The interval $0 \leqslant y \leqslant h_i$ is the range of definition of the boundary condition; it is also the range of orthogonality of the modes with $q_{i,m}(y)$, therefore, the integral operator is applied on both sides of equation (11b)

$$\frac{1}{h_i}\int_0^{h_i} \ldots\ldots \cdot q_{i,m}(y)\, \mathrm{d}y, \tag{12}$$

and the linear system of equations ($m = 0, 1, 2, \ldots$)

$$(A_{i,m} + B_{i,m}\, \mathrm{e}^{-\gamma_{i,m}\Delta x}) N_{i,m} = \sum_n (A_{i-1,n}\, \mathrm{e}^{-\gamma_{i-1,n}\Delta x} + B_{i-1,n}) C(i,m; i-1, n), \tag{13}$$

are obtained. It is an upward iteration scheme in i for the two sets of amplitudes $\{A_{i,m}\}$, $\{B_{i,m}\}$.

The boundary condition for the axial component of the particle velocity at the entrance $x = x_{i-1}$ of the ith section ($i \geqslant 1$) is

$$vx_{e,i-1}(x_{i-1}, y) + vx_{r,i-1}(x_{i-1}, y) \stackrel{!}{=} \begin{Bmatrix} 0, & h_i \leqslant y \leqslant h_{i-1} \\ vx_{e,i}(x_{i-1}, y) + vx_{r,i}(x_{i-1}, y), & 0 \leqslant y \leqslant h_i \end{Bmatrix}. \tag{14}$$

On the right side of equation (14), it is assumed that the head of the step in the interval $h_i \leqslant y \leqslant h_{i-1}$ is rigid. This assumption is reasonable for locally reacting

absorbers which do not support sound oscillations parallel to their surface. However, it should not be overlooked that a rigid head of a step is an artefact of our model of approximation to the wedge by stepped duct sections; the influence of the heads will become negligible with an increasing number of steps. The boundary condition for the particle velocity is

$$\sum_m (A_{i-1,m}\,\mathrm{e}^{-\gamma_{i-1,m}\Delta x} - B_{i-1,m})\gamma_{i-1,m}q_{i-1,m}(y)$$

$$\stackrel{!}{=} \begin{cases} 0, & h_i \leqslant y \leqslant h_{i-1} \\ \sum_m (A_{i,m} - B_{i,m}\,\mathrm{e}^{-\gamma_{i,m}\Delta x})\gamma_{i,m}q_{i,m}(y), & 0 \leqslant y \leqslant h_i \end{cases}. \quad (15)$$

Now the range of the boundary condition is the wider range $0 \leqslant y \leqslant h_{i-1}$. It would be normal, therefore, to apply an orthogonality integral like expression (12), but now in the wider range $i-1$, i.e., on the other side of the entrance plane as compared to expression (12). This "two-sided" orthogonality, however, would produce a downward iteration scheme, and the numerical solution of the two iteration schemes (each in a different direction) would run into problems with ill-conditioned matrices when the number I of sections is not very low (see below for more about this point). Although experience shows that the precision of a "two-sided" orthogonality is somewhat higher than that of a "one-sided" orthogonality for a small number of sections, the same orthogonality integral as in expression (12) is applied on the lower line on the right side of equation (15). On the left side of equation (15), the zero value of the particle velocity in $h_i \leqslant y \leqslant h_{i-1}$ is taken into consideration and the integral is extended up to h_{i-1}; thus, one applies

$$\frac{1}{h_i}\int_0^{h_i} \ldots \cdot q_{i,m}(y)\,\mathrm{d}y \quad \text{right}, \qquad \frac{1}{h_i}\int_0^{h_{i-1}} \ldots \cdot q_{i,m}(y)\,\mathrm{d}y \quad \text{left}. \quad (16)$$

The rigid step head is thus considered implicitly. These operations will give the system of equations

$$(A_{i,m} - B_{i,m}\,\mathrm{e}^{-\gamma_{i,m}\Delta x})\gamma_{i,m}N_{i,m} = \frac{h_{i-1}}{h_i}\sum_n (A_{i-1,n}\,\mathrm{e}^{-\gamma_{i-1,n}\Delta x} - B_{i-1,n})\gamma_{i-1,n}C(i-1,n;i,m). \quad (17)$$

The boundary conditions at the exit plane $x = x_i$ of the ith section lead to systems of equations which would be obtained from equations (13) and (17) by the replacement $i \to i+1$.

From the combination of equations (13) and (17), one gets

$$A_{i,m} = \frac{1}{2N_{i,m}} \sum_n A_{i-1,n}\, \mathrm{e}^{-\gamma_{i-1,n}\Delta x}\left(C(i,m;\, i-1,\, n) + C(i-1,\, n;\, i,\, m)\, \frac{\gamma_{i-1,n} h_{i-1}}{\gamma_{i,m} h_i} \right)$$

$$+\ B_{i-1,n}\left(C(i,m;\, i-1,\, n) - C(i-1,\, n;\, i,\, m)\, \frac{\gamma_{i-1,n} h_{i-1}}{\gamma_{i,m} h_i} \right), \tag{18}$$

$$B_{i,m} = \frac{1}{2N_{i,m}\, \mathrm{e}^{-\gamma_{i,m}\Delta x}} \sum_n A_{i-1,n}\, \mathrm{e}^{-\gamma_{i-1,n}\Delta x}\left(C(i,m;\, i-1,\, n) - C(i-1,\, n;\, i,\, m)\, \frac{\gamma_{i-1,n} h_{i-1}}{\gamma_{i,m} h_i} \right)$$

$$+\ B_{i-1,n}\left(C(i,m;\, i-1,\, n) + C(i-1,\, n;\, i,\, m)\, \frac{\gamma_{i-1,n} h_{i-1}}{\gamma_{i,m} h_i} \right), \tag{19}$$

These are two upward iteration schemes in i. The schemes begin at $i = 1$. Then the $A_{i-1,m}$ on the left sides are the known amplitudes $A_{0,m}$ of the incident modes; the terms, including them, are purely numerical. $B_{0,m}$ on the left sides are unknown and remain symbolic quantities. At any step i of the iteration, one will have systems of equations of the form

$$A_{i,m} = \sum_n a_{i,n} + b_{i,n} B_{0,n}, \qquad B_{i,m} = \sum_n \alpha_{i,n} + \beta_{i,n} B_{0,n}, \tag{20}$$

with purely numerical $a_{i,n}$, $b_{i,n}$, $\alpha_{i,n}$, $\beta_{i,n}$. Such a mixed numerical and symbolic computation can easily be performed with computer programs for numerical and symbolic computations (such as *Mathematica*). In a purely numerical computing frame (such as FORTRAN) the transformations from equations (18) and (19) to equation (20) must be explicitly formulated. The iteration ends with $i = I$ where on the left sides of equations (18) and (19) stand $\{A_{I,m}\}$ and $\{B_{I,m}\}$ which, with equation (8), reduces to only the $\{A_{I,m}\}$, which are yet unknown. Thus equations (20) are for $i = I$ two linear systems of equations in the two sets of amplitudes $\{A_{I,m}\}$, $\{B_{0,n}\}$, and are inhomogeneous systems of equations because of the numerical terms $a_{I,n}$, $\alpha_{I,n}$. After they are solved for $\{B_{0,n}\}$, all amplitudes $\{A_{i,m}\}$, $\{B_{i,m}\}$ can be evaluated by insertion. Thus, the task of the field computation in a converging wedge is completed.

5. MODAL ANALYSIS IN THE DIVERGING WEDGE

The boundary condition for the sound pressure at the entrance $x = x_{i-1}$ of the ith section now is

$$p_{e,i-1}(x_{i-1},\, y) + p_{r,i-1}(x_{i-1},\, y) \stackrel{!}{=} p_{e,i}(x_{i-1},\, y) + p_{r,i}(x_{i-1},\, y), \qquad 0 \leqslant y \leqslant h_{i-1}, \tag{21}$$

which with the field formulations reads

$$\sum_m (A_{i-1,m}\,\mathrm{e}^{-\gamma_{i-1,m}\Delta x} + B_{i-1,m})q_{i-1,m}(y) \stackrel{!}{=} \sum_m (A_{i,m} + B_{i,m}\,\mathrm{e}^{-\gamma_{i,m}\Delta x})q_{i,m}(y). \tag{22}$$

The application of integral operator

$$\frac{1}{h_{i-1}}\int_0^{h_{i-1}} \ldots . \cdot\, q_{i-1,m}(y)\,\mathrm{d}y \tag{23}$$

on both sides gives the system of equations ($m = 0, 1, \ldots$)

$$(A_{i-1,m}\,\mathrm{e}^{-\gamma_{i-1,m}\Delta x} + B_{i-1,m})N_{i-1,m} = \sum_n (A_{i,n} + B_{i,n}\,\mathrm{e}^{-\gamma_{i,n}\Delta x})C(i-1, m; i, n). \tag{24}$$

The boundary condition for the axial particle velocity at the entrance $x = x_{i-1}$ of the ith section is

$$vx_{e,i}(x_{i-1}, y) + vx_{r,i}(x_{i-1}, y) \stackrel{!}{=} \begin{Bmatrix} 0, & h_{i-1} \leqslant y \leqslant h_i \\ vx_{e,i-1}(x_{i-1}, y) + vx_{r,i-1}(x_{i-1}, y), & 0 \leqslant y \leqslant h_{i-1} \end{Bmatrix}. \tag{25}$$

Here again the orthogonality integral is applied on the narrow section $i-1$ (i.e., on the second line of the right side of equation (25)) and it is extended from h_{i-1} to h_i on the left side, thus taking into consideration the vanishing particle velocity at the head of the step. That is, one applies

$$\frac{1}{h_{i-1}}\int_0^{h_{i-1}} \ldots . \cdot\, q_{i-1,m}(y)\,\mathrm{d}y \quad \text{right}, \qquad \frac{1}{h_{i-1}}\int_0^{h_i} \ldots . \cdot\, q_{i-1,m}(y)\,\mathrm{d}y \quad \text{left}, \tag{26}$$

and obtains

$$(A_{i-1,m}\,\mathrm{e}^{-\gamma_{i-1,m}\Delta x} - B_{i-1,m})\gamma_{i-1,m}N_{i-1,m} = \frac{h_i}{h_{i-1}}\sum_n (A_{i,n} - B_{i,n}\,\mathrm{e}^{-\gamma_{i,n}\Delta x})\gamma_{i,n}C(i, n; i-1, m). \tag{27}$$

Both systems of equations (24) and (27) are downward iterations in i, which, when evaluated for individual amplitudes, can be written as

$$A_{i-1,m} = \frac{1}{2N_{i-1,m}\,\mathrm{e}^{-\gamma_{i-1,m}\Delta x}}\sum_n A_{i,n}\left(C(i-1, m; i, n) + \frac{\gamma_{i,n}h_i}{\gamma_{i-1,m}h_{i-1}}\,C(i, n; i-1, m)\right)$$

$$+\, B_{i,n}\,\mathrm{e}^{-\gamma_{i,n}\Delta x}\left(C(i-1, m; i, n) - \frac{\gamma_{i,n}h_i}{\gamma_{i-1,m}h_{i-1}}\,C(i, n; i-1, m)\right), \tag{28}$$

$$B_{i-1,m} = \frac{1}{2N_{i-1,m}} \sum_n A_{i,n} \left(C(i-1, m; i, n) - \frac{\gamma_{i,n} h_i}{\gamma_{i-1,m} h_{i-1}} C(i, n; i-1, m) \right)$$

$$+ B_{i,n} \, \mathrm{e}^{-\gamma_{i,n} \Delta x} \left(C(i-1, m; i, n) + \frac{\gamma_{i,n} h_i}{\gamma_{i-1,m} h_{i-1}} C(i, n; i-1, m) \right). \quad (29)$$

When one begins the iteration with $i = I$, the equations have the form

$$A_{I-1,m} = \sum_n b_{I,n} A_{I,n}, \qquad B_{I-1,m} = \sum_n \beta_{I,n} A_{I,n}, \quad (30a)$$

with still unknown amplitudes $\{A_{I,n}\}$, and, in the general step i,

$$A_{i-1,m} = \sum_n b_{i,n} A_{I,n}, \qquad B_{i-1,m} = \sum_n \beta_{i,n} A_{I,n}, \quad (30b)$$

with numerical values of the $b_{i,n}$ and $\beta_{i,n}$. At the end with $i = 1$, one has the known amplitudes $\{A_{0,m}\}$ of the incident modes on the left side of the first line in equation (30b). Thus, it can be solved for the $\{A_{I,n}\}$ and with these all other amplitudes $\{A_{i,m}\}$, $\{B_{i,m}\}$ are computed by insertion.

6. NUMERICAL EXAMPLES

Before a few numerical examples are shown, some remarks should be made which relate to the amount and precision of the numerical computations. The computations in the previous section about the diverging wedge evidently are simpler than for the converging wedge in section 4 (no mixed numerical and symbolic terms in equation (30b), only a simple system of equations to be solved at the end of the iteration instead of a couple of systems of equations). However, the assumption of symbolic amplitudes $\{A_{I,n}\}$ in fact means the assumption of about unit values for these amplitudes during the iteration, which may be in error to the final values of the $\{A_{I,n}\}$ by orders of magnitude; the final equation to be solved may become badly conditioned for the numerical solution if the upper limit m_{hi} of the mode orders is assumed unnecessarily high. The next remark concerns the number I of steps. It is known from many numerical and experimental examples in the literature of approximations of steady variations of parameters in sound fields by parameter steps that the number I of steps should not be too low. As a rule of thumb, one should remain below $k_0 \Delta y \approx 0{\cdot}35$. An upper limit for $k_0 \Delta y$ is also set by the algorithm for the solution of the characteristic equation. Under the condition that $k_0 h_i G$ does not pass too close to one of the branch points of the transformation defined by the characteristic equation, $k_0 \Delta y \approx 0{\cdot}35$ is an upper limit also in this respect. If one of the $k_0 h_i G$ approaches a branch point, the step $k_0 \Delta y$ must be selected with a smaller value.

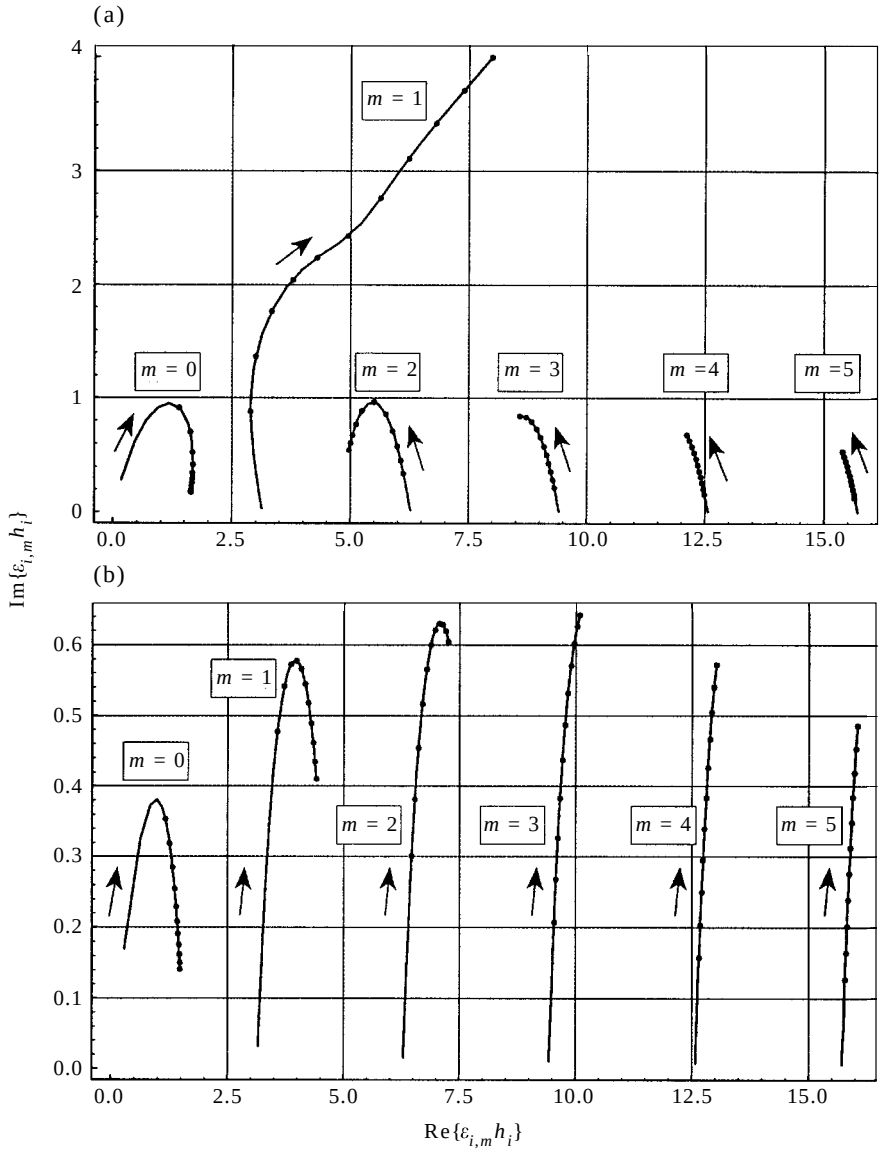

Figure 2. (a) Lateral wave nunbers $\varepsilon_{i,m}h_i$ of the six lowest modes $m = 0, \ldots, 5$ for the wall admittance $G = 2 + \mathrm{j}$. The points are stepped with $k_0\Delta h = 0{\cdot}3$ between $k_0h = 1$ and $k_0h = 4$; the directions for increasing k_0h are indicated. (b) as (a), but with the wall admittance $G = 2 - \mathrm{j}$.

A further remark concerns different formally possible ways in which the modal analysis could be performed. It was mentioned above that the application of a "two-sided" orthogonality produces better precision when applied to field transformations by just one intermediate section, but it cannot be applied in the case of many sections. This aspect is illustrated for the converging wedge. The boundary condition, equations (14) and (15), for the axial component of the particle velocity at the entrance $x = x_{i-1}$ of the ith section would be transformed

to a system of equations for the amplitudes with a two-sided orthogonality by the application of the integrals

$$\frac{1}{h_{i-1}}\int_0^{h_{i-1}} \ldots . \cdot q_{i-1,m}(y)\,\mathrm{d}y \quad \text{left}, \qquad \frac{1}{h_{i-1}}\int_0^{h_i} \ldots . \cdot q_{i-1,m}(y)\,\mathrm{d}y \quad \text{right} \quad (31)$$

on both sides of equation (15), where the reduction of the upper limit $h_{i-1} \to h_i$ is demanded by the vanishing particle velocity at the head of the step. This leads to the system of equations

$$(A_{i-1,m}\,\mathrm{e}^{-\gamma_{i-1,m}\Delta x} - B_{i-1,m})\gamma_{i-1,m} = \frac{h_i}{h_{i-1}}\sum_n (A_{i,n} - B_{i,n}\,\mathrm{e}^{-\gamma_{i,n}\Delta x})\gamma_{i,n} C(i, n; i-1, m). \quad (32)$$

which is applied in combination with the system of equations (13). The directions of both iteration schemes are opposite to each other. The direction of iteration of system (13) can be changed by its formal solution when it is written as a matrix equation,

$$\{A_{i-1,m}\,\mathrm{e}^{-\gamma_{i-1,m}\Delta x} + B_{i-1,m}\} = \left\{\frac{C(i, n; i-1, m)}{N_{i,n}}\right\}^{-1} \circ \{A_{i,n} + B_{i,n}\,\mathrm{e}^{-\gamma_{i,n}\Delta x}\}\,, \quad (33a)$$

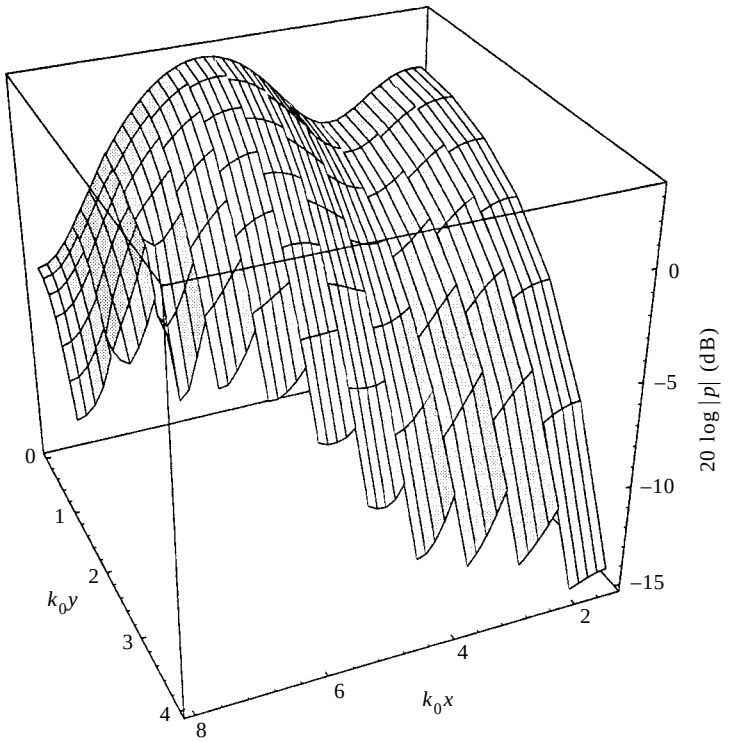

Figure 3. Sound pressure level 20 log $|p|$ in a converging wedge with a wall admittance $G = 2 - \mathrm{j}$ excited by the fundamental mode $m = 0$ of the entrance duct. $G_t = 4$, $m_{hi} = 5$, $I = 10$, $\Delta x/\Delta y = 0{\cdot}5$, $h_0 \Delta h_i = 0{\cdot}3$, $\{A_{0,m}\} = \{1, 0, 0, 0, 0, 0\}$.

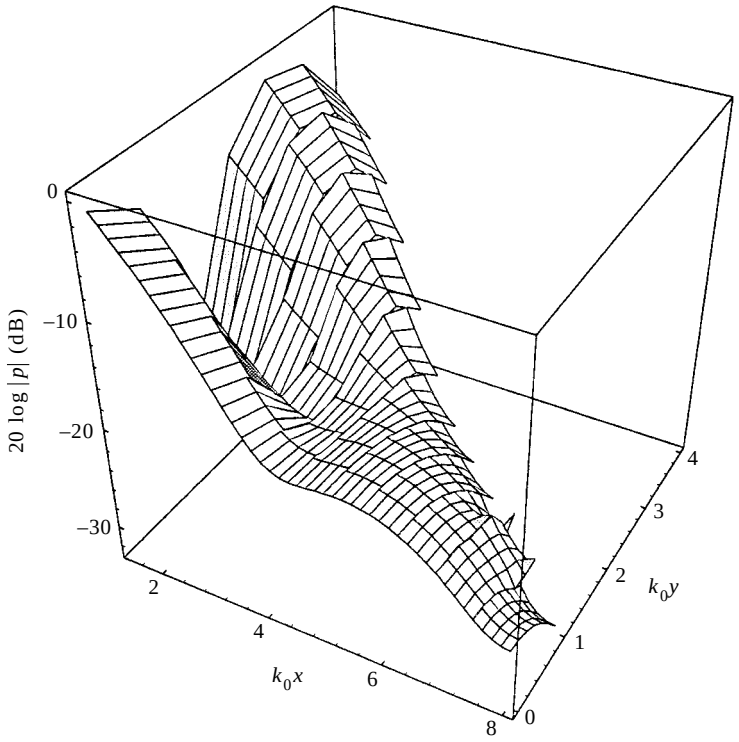

Figure 4. As Figure 3, but now with the first higher mode $m = 1$ as the incident mode.

which is combined with equation (32) in matrix form:

$$\{A_{i-1,m}\,\mathrm{e}^{-\gamma_{i-1,m}\Delta x} - B_{i-1,m}\} = \left\{\frac{C(i,n;i-1,m)\gamma_{i,n}h_i}{N_{i-1,m}\gamma_{i-1,m}h_{i-1}}\right\} \circ \{A_{i,n} - B_{i,n}\,\mathrm{e}^{-\gamma_{i,n}\Delta x}\}. \tag{33b}$$

In equation (33a), $\{\ldots\}^{-1}$ means the inverse of a matrix for left side multiplication. So one gets iterations in one direction (downwards) for the two sets of amplitudes:

$$\{A_{i-1,m}\} = \frac{1}{2\,\mathrm{e}^{-\gamma_{i-1,m}\Delta x}}\left[\left\{\frac{C(i,n;i-1,m)}{N_{i,n}}\right\}^{-1} + \left\{\frac{C(i,n;i-1,m)\gamma_{i,n}h_i}{N_{i-1,m}\gamma_{i-1,m}h_{i-1}}\right\}\right] \circ \{A_{i,n}\}$$

$$+ \frac{\mathrm{e}^{-\gamma_{i,n}\Delta x}}{2\,\mathrm{e}^{-\gamma_{i-1,m}\Delta x}}\left[\left\{\frac{C(i,n;i-1,m)}{N_{i,n}}\right\}^{-1}\right.$$

$$\left. - \left\{\frac{C(i,n;i-1,m)\gamma_{i,n}h_i}{N_{i-1,m}\gamma_{i-1,m}h_{i-1}}\right\}\right] \circ \{B_{i,n}\}, \tag{34a}$$

$$\{B_{i-1,m}\} = \frac{1}{2}\left[\left\{\frac{C(i,n;i-1,m)}{N_{i,n}}\right\}^{-1} - \left\{\frac{C(i,n;i-1,m)\gamma_{i,n}h_i}{N_{i-1,m}\gamma_{i-1,m}h_{i-1}}\right\}\right] \circ \{A_{i,n}\}$$

$$+ \frac{\mathrm{e}^{-\gamma_{i,n}\Delta x}}{2}\left[\left\{\frac{C(i,n;i-1,m)}{N_{i,n}}\right\}^{-1}\right.$$

$$\left. + \left\{\frac{C(i,n;i-1,m)\gamma_{i,n}h_i}{N_{i-1,m}\gamma_{i-1,m}h_{i-1}}\right\}\right] \circ \{B_{i,n}\}. \tag{34b}$$

The problems with this formally correct solution begin during the numerical computations. The matrix $\{C(i,n;i-1,m)/N_{i,n}\}$ is approximately tri-diagonal (modes of one duct section mainly couple with modes of the same order in the adjacent section). The off-diagonal elements of the inverse matrix therefore have high magnitudes, and the inverse matrices are multiplied iteratively. Thus, the final system of equations becomes extremely badly conditioned for a numerical solution, if the object consists of many duct sections.

In the following numerical examples, k_0x, k_0y are taken as the local variables (for a fixed frequency) which allows one to let the wave numbers appear in the forms $\varepsilon_{i,m}h_i$, $\gamma_{i,m}h_i$ as they are produced by the characteristic equation (5) and by

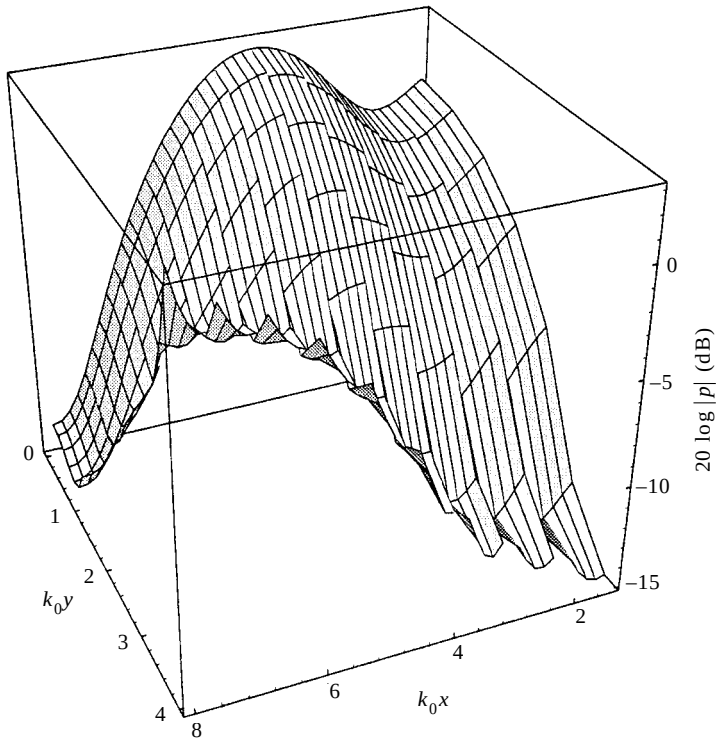

Figure 5. Sound pressure level 20 log $|p|$ in a converging wedge with a wall admittance $G = 2 + \mathrm{j}$ excited by the fundamental mode $m = 0$ of the entrance duct. Other parameters as Figure 3.

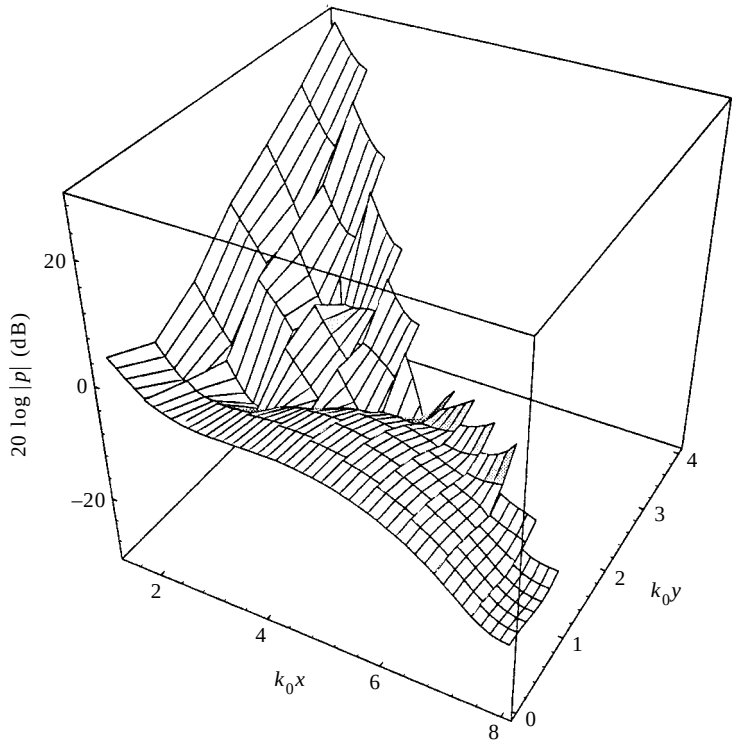

Figure 6. As Figure 5, but now with the first higher mode $m = 1$ as the incident mode; this is the surface wave mode in the entrance duct.

the secular equation (4). One then has to select values for the tangent of the wedge angle $\tan \alpha = \Delta y/\Delta x$ and for the admittances G and G_t. Take $\tan \alpha = 0{\cdot}5$ and the two values $G = 2 \pm \mathrm{j}$ together with $G_t = 1$, which represents full absorption for a normal plane wave incidence on the termination (but finite reflections for incident modes) and thus represents a termination of the wedge by an infinitely long rigid duct. The widths are selected as $k_0h_0 = 4$ and $k_0h_I = 1$ for the converging wedge, and $k_0h_0 = 1$ and $k_0h_I = 4$ for the diverging wedge. The number of steps is $I = 10$ which gives $k_0\Delta y = 0{\cdot}3$.

Figures 2(a, b) show the lateral wave numbers $\varepsilon_{i,m}h_i$ in their complex plane for $m = 0, 1, \ldots, 5$ and k_0h varied between 0·05 and 4 for the curves and between 1 and 4 in steps of $k_0\Delta h = 0{\cdot}3$ for the points (which are the steps in the field computations below). The admittance values in the diagrams are $G = 2 \pm \mathrm{j}$, respectively. The arrows at the curves show the direction of increasing k_0h. The mode $m = 1$ with $G = 2 + \mathrm{j}$ (spring type reactance of the absorber) is the surface wave mode. If a surface wave mode exists, then the modes with lower and higher orders, respectively, than the order of the surface wave mode have opposite curvatures for increasing k_0h.

We begin the presentation of sound pressure levels ($20 \log |p|$ is plotted in the vertical direction of the diagrams) in the *converging* wedge. The excitation mode in Figure 3 is the mode $m = 0$ of the duct ahead of the wedge with unit amplitude $A_{0,0} = 1$. The angle of the wedge is given by $\tan \alpha = \Delta y/\Delta x = 0{\cdot}5$. The wall

admittance is $G = 2 - \mathrm{j}$; the other parameters are indicated in the diagram. $I = 10$ duct sections plus a section of the entrance duct are displayed along the axial co-ordinate $k_0 x$. The imperfections of the field fitting at the section limits mainly comes from the relatively large steps $\Delta k_0 y$ of the field sampling points in the lateral direction (six sampling points in the interval $0 \leqslant k_0 y \leqslant k_0 h_i$) and from the fact that the sampling points do not coincide on both sides of a section limit. The modal pattern (shape of the lateral profile) changes only marginally during the propagation in the wedge. The local attenuation changes as a consequence of internal reflections in the wedge. The overall transmission loss in a two-sided wedge (both boundaries inclined and lined) with a length equal to the width at the entrance is about 8 dB.

The next level plot in Figure 4 is for a wedge as in Figure 3; only the mode order of the single incident mode is increased to $m = 1$ (the point of view is changed compared to Figure 3). Now the mode pattern drastically changes during the propagation in the wedge: whereas the pattern at the entrance corresponds to the first higher mode, it takes the form of the fundamental mode at the exit. Corresponding to this change of the dominant mode is the strong change in the local attenuation. The overall transmission loss (of about 27 dB) is mainly produced in the local range of the dominant higher mode.

In Figure 5 (still for a converging wedge) the order of the incident mode is again $m = 0$, but now the wall admittance is changed to $G = 2 + \mathrm{j}$. The change of the

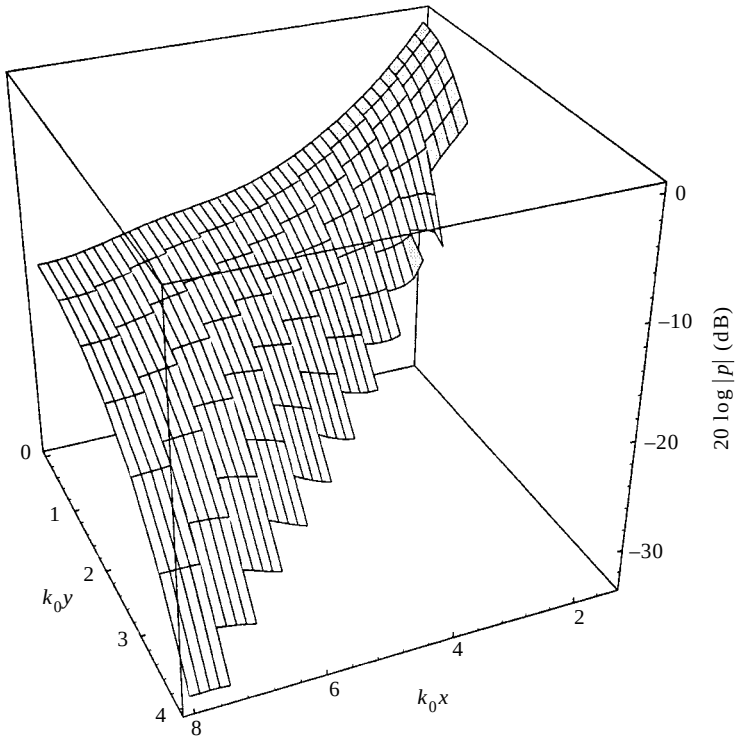

Figure 7. Sound presure level in a diverging wedge with a wall admittance $G = 2 - \mathrm{j}$ and the fundamental mode $m = 0$ of the entrance duct as exciting mode. Other parameters as Figure 3.

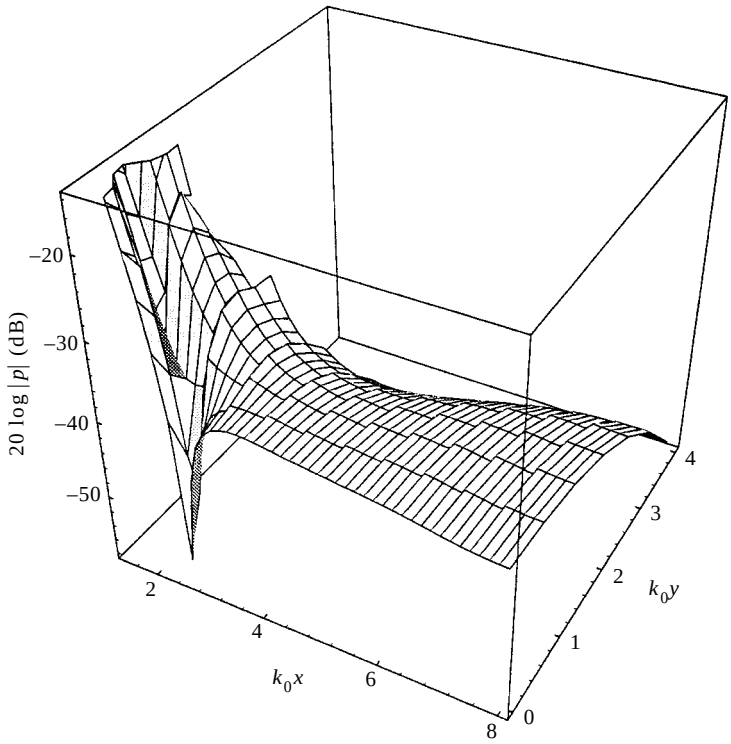

Figure 8. As Figure 7, but now with the first higher mode $m = 1$ as the exciting mode.

field pattern in the lateral direction is stronger with this admittance than with that of Figure 3; the overall transmission loss correspondingly is increased to about 15 dB. The internal reflections in the wedge are visible from the axial standing wave distribution.

In Figure 6, the sound pressure level is shown for the wedge of Figure 5, but now the mode order of the incident mode is increased to $m = 1$ (and the point of view is changed). As can be seen from Figure 2(a), the incident mode at the entrance into the wedge is the surface wave mode (with an exponential decay away from the absorber surface). This character of the sound field is retained only over a few sections of the wedge; in later sections the field pattern changes over to the pattern of the dominant fundamental mode. The field matching at the first section limits is not so good as in the previous diagrams; the number of modes involved in the modal analysis should be increased with the incident surface wave mode beyond the limit $m_{hi} = 5$ applied here; this is a general finding, because many normal modes are needed for the synthesis of the exponential slope of the surface wave mode.

The next diagrams are for a *diverging* wedge. The diagrams also show the sound pressure level over k_0x, k_0y. The parameter combinations are similar to those in the previous diagrams for the converging wedge.

Figure 7 is for a diverging wedge with a wall admittance $G = 2 - \mathrm{j}$ and the incident fundamental mode $m = 0$. The field pattern retains its modal character;

internal reflections practically do not exist. The local attenuation is inversely proportional to the local width.

In Figure 8, the mode order of the incident mode is increased relative to Figure 7 to $m = 1$ (and the point of view is different). The field pattern changes from that of the dominant higher mode near the entrance to that of the fundamental mode near the exit. The total transmission loss is produced in the range of the higher mode in the first two wedge sections. The change of the dominant mode is also visible from the deep interference minimum.

Figure 9 is a sound pressure level plot in a diverging wedge with a wall admittance $G = 2 + \mathrm{j}$ excited by the fundamental mode $m = 0$ of the entrance duct. The change during propagation of the lateral profile corresponds to the change of the profile of the fundamental mode in narrow to wide ducts; mode conversion practically does not occur.

Figure 10 corresponds to Figure 9 except for the increase in the mode order of the exciting mode to $m = 1$. The surface wave character of the exciting mode is not yet fully developed in the narrow entrance duct with $k_0 h_0 = 1$. Therefore, the transition of the modal pattern along the wedge is not so pronounced, as in the converging wedge with the wider entrance duct having a value $k_0 h_0 = 4$. Nevertheless, the local attenuation concentrates on the range with the dominant higher mode.

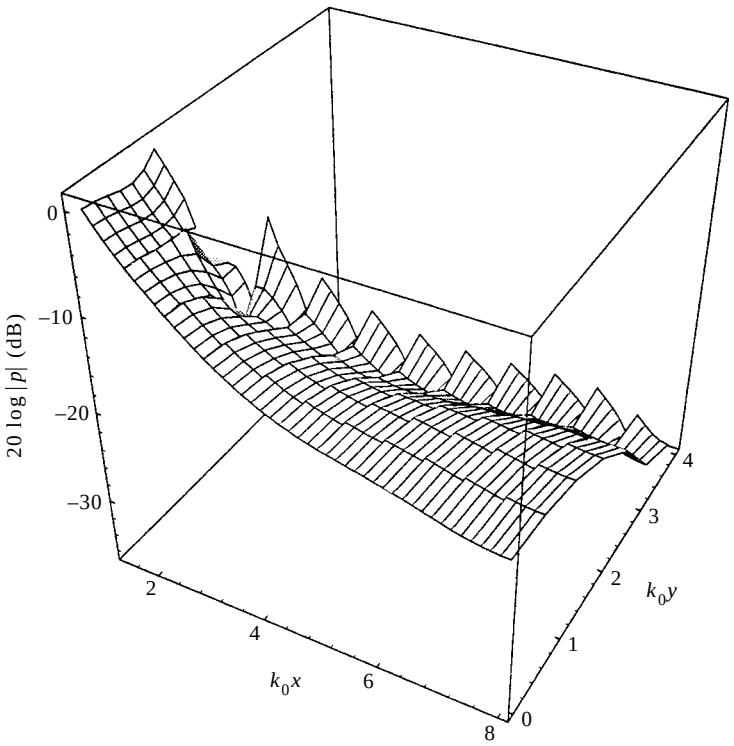

Figure 9. Sound pressure level in a diverging wedge with a wall admittance $G = 2 + \mathrm{j}$ and the fundamental mode $m = 0$ of the entrance duct as exciting mode. Other parameters as Figure 3.

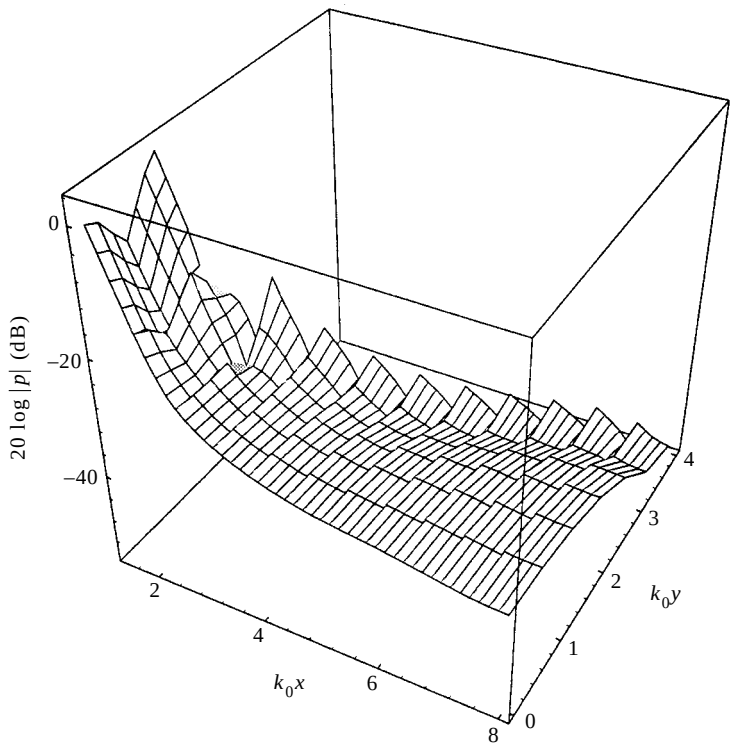

Figure 10. As Figure 9, but with the first higher mode $m = 1$ as the exciting mode.

7. RIGID WEDGE-SHAPED DUCT TRANSITIONS

It is of some practical interest to compare the numerical results of the previous section for lined wedge-shaped duct transitions with similar results for wedge-shaped transitions with rigid walls, because such rigid wall transitions are practically always associated with splitter type silencers in a duct system. One has only to set $G \rightarrow 0$ for the production of numerical examples. In fact G is set to a small complex value, in order to avoid numerical singularities, $G = 0{\cdot}01 - 0{\cdot}01\mathrm{j}$. This value would approximately correspond to the viscous losses and to the mass reactance at a metal sheet wall.

Figure 11 shows the sound pressure level in a (nearly) rigid *converging* duct transition for the plane wave as the incident mode. The incident plane wave mainly couples to the first higher mode of the wide wedge sections near the entrance (which there is a propagating mode). This change of the dominant mode is accompanied by strong internal interference variations. Deeper in the wedge the higher mode couples back to the plane wave. As an overall effect, the sound pressure level at the exit is higher than at the entrance by about the ratio of the end areas.

If the exciting mode for the converging, nearly rigid wedge is the first higher mode $m = 1$ of the (nearly) rigid entrance duct, as in Figure 12, the exciting mode runs into cut-off conditions inside the wedge. The approach to cut-off is associated

with a remarkable level reduction. Behind the cut-off section of the incident mode the fundamental mode $m = 0$ is dominant.

In Figure 13, the (nearly) rigid wedge is *diverging* and is excited by an incident plane wave. Although the internal reflections produce some higher mode content of the field, the plane wave remains the dominant mode and the reduction of the sound pressure level corresponds to the increase of the local duct area in the wedge.

Figure 14 corresponds to Figure 13 (rigid diverging wedge), except the incident mode is the first higher mode $m = 1$ of the entrance duct, which there is a cut-off mode. Therefore, this case is only of principal interest inasmuch as it shows that the tendency of mode conversion in a wedge is in the direction of lower mode orders; the mode $m = 1$ is a propagating mode near the exit of the wedge, however, the dominant mode there is $m = 0$.

It is this—not at all trivial—fact which explains the common experience that computations of the transmission loss of splitter type silencers which are performed with entrance and exit ducts having the same widths as the silencer and with an incident plane wave agree quite well with measured data taken at silencers which are preceded and followed by conical rigid duct transitions.

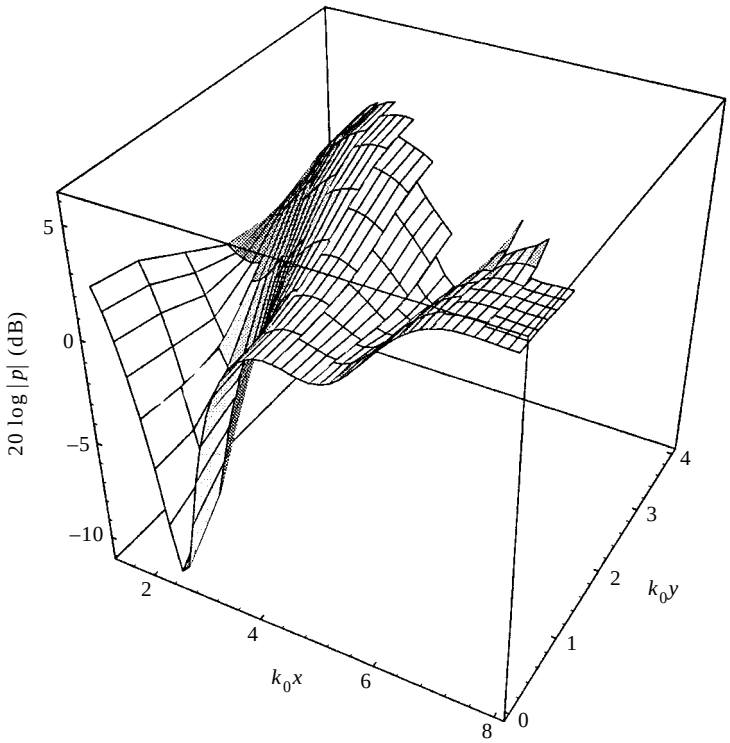

Figure 11. Sound pressure level in a converging wedge-shaped duct transition with (nearly) rigid walls for an incident plane sound wave. $G = 0{\cdot}01 - 0{\cdot}01\mathrm{j}$, $G_t = 1$, $\mathrm{m_h} = 5$, $I = 10$, $\Delta x/\Delta y = 0{\cdot}5$, $k_0 h_i = 0{\cdot}3$, $\{A_{0,m}\} = \{1, 0, 0, 0, 0, 0\}$.

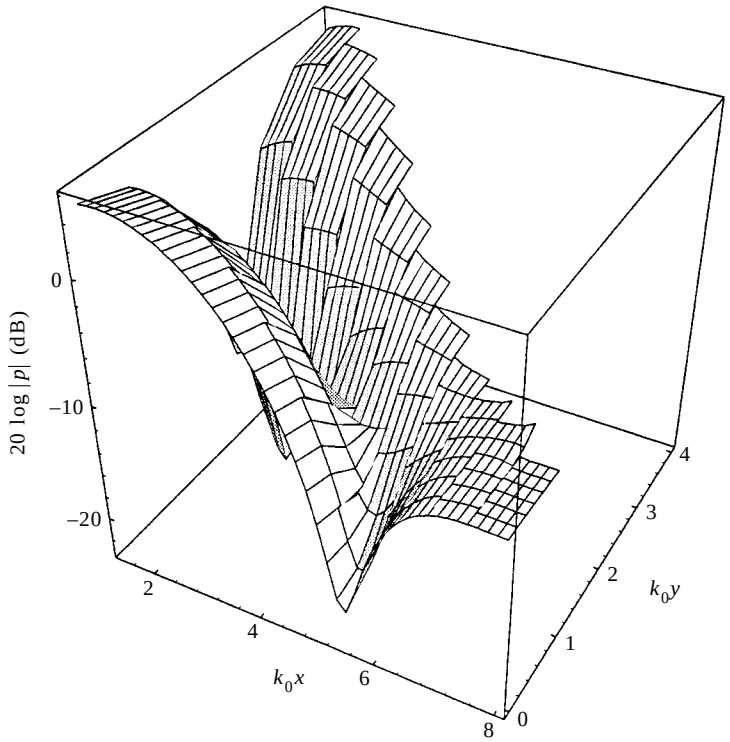

Figure 12. As Figure 11, but excited by the first higher mode of the rigid entrance duct.

8. CONCLUDING REMARKS

Conical transitions are unavoidable between the flow ducts and inserted splitter type silencers, and they are advantageous between the sections of silencer cascades with different duct widths. The computation of the total transmission loss of such silencer installations, including all modal reflections and couplings, needs an algorithm for the evaluation of the sound transmission through wedge-shaped duct sections. The few examples shown above indicate that it is reasonable to apply sound absorbing linings at the walls of the transitions. Three global effects can be distinguished: the internal reflections in the converging wedge, the coupling to other dominant modes, mostly lower in the mode order, and the variation of the local attenuation corresponding to the changing local duct width.

The computation of a sound pressure level plot, as shown above, took about 2 min (with non-compiled *Mathematica* programs on a Macintosh Quadra 800). Most of the time is consumed by the evaluation of the mode amplitudes of the internal sections and by the computation of the sound field at the sampling points. In a silencer design neither the internal mode amplitudes are needed (only the $B_{0,m}$ and $A_{I,m}$ are used in further computations) nor the sound pressure value in internal spatial points.

The choice of the same wall admittance value G for the lining of the entrance duct (section $i = 0$) as for the other sections of the transition wedge is not mandatory. If a different value G_0 is taken for the entrance duct, only the wave

numbers $\varepsilon_{0,m}h_0$ and the propagation constants $\gamma_{0,m}h_0$ must be evaluated separately; the remainder of the procedure remains the same It is not even necessary that the lining admittance G is constant along the wedge; a variable $G(x)$ would have only the consequence that the characteristic equation must be solved for a number of right sides.

As was already mentioned above, the use of a locally reacting lining is only a matter of simplicity. A similar modal analysis with the somewhat more complicated orthogonality relation of modes in a duct with a bulk reacting lining can be performed. Examples of modal analysis computations in ducts with bulk reacting linings are included in reference [2].

Above it was assumed tacitly that the wedge extends infinitely in the z direction (direction normal to the planes of Figures 1(a) and 1(b)) and that the sound field is constant in that direction. In the case of a finite extend in the z direction and/or of a sound source producing a sound field with a z profile $q_z(z)$, one would have to multiply all field components in equations (1) and (2) by $q_z(z)$. This factor would cancel in the above computations (except in the plots for the field). If $q_z(z)$ is proportional to one of the distributions $e^{\pm jk_z z}$, $\cos(k_z z)$ and $\sin(k_z z)$ with a given wave number k_z or to a linear combination of them and if the walls terminating the wedge in the z direction are parallel to each other, the only consequence would

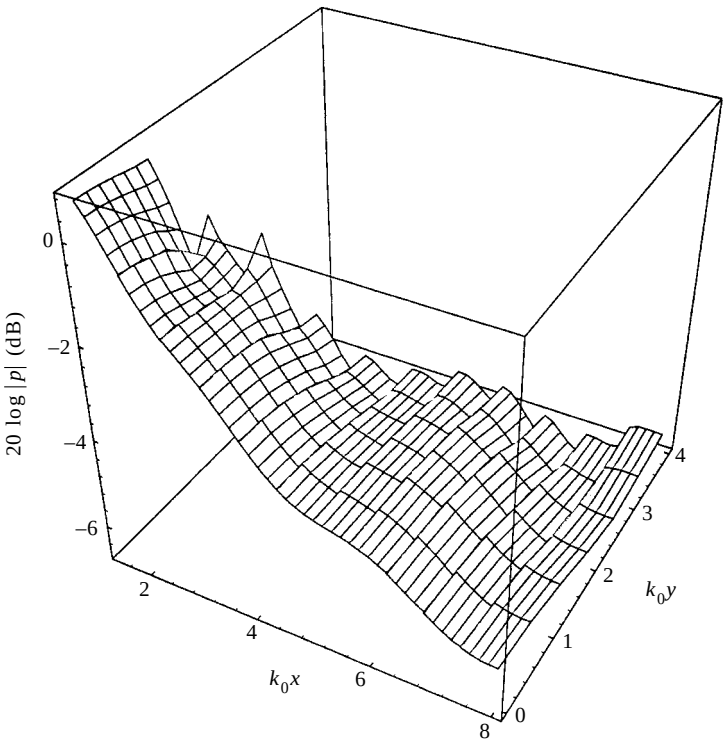

Figure 13. Sound pressure level in a (nearly) rigid diverging wedge-shaped duct transition with the plane wave as exciting mode. $G = 0{\cdot}01 - 0{\cdot}01\mathrm{j}$, $G_t = 1$, $m_{hi} = 5$, $I = 10$, $\Delta x/\Delta y = 0{\cdot}5$, $k_0\Delta h_i = 0{\cdot}3$, $\{A_{0,m}\} = \{1, 0, 0, 0, 0, 0\}$.

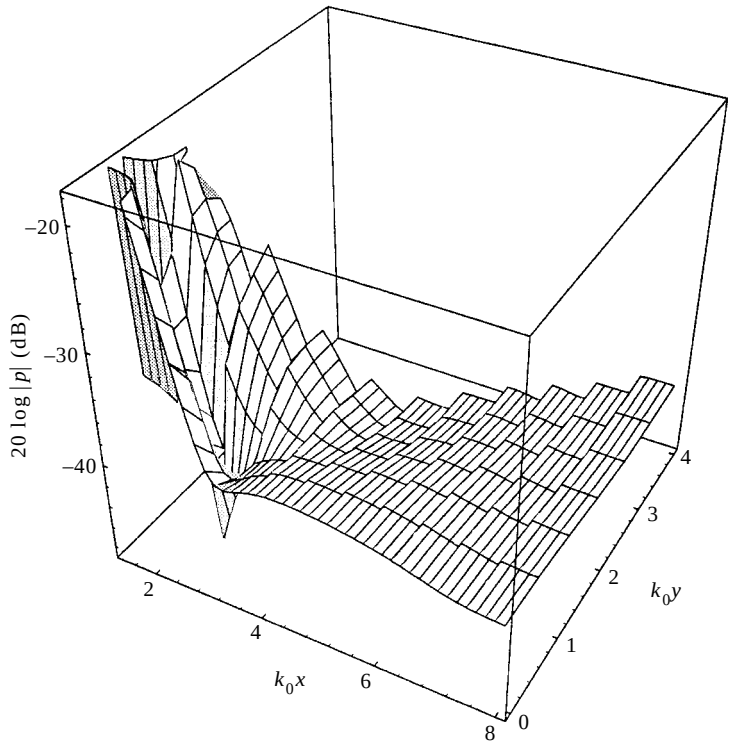

Figure 14. As Figure 13, but excited by the first higher mode $m = 1$ of the entrance duct, which there is a cut-off mode.

be the replacement $k_0^2 \rightarrow k_0^2 - k_z^2$ in equation (4). Thus, a sound source and/or a termination of the wedge by lateral, parallel walls (either rigid or absorbing) can be easily introduced. If the sound field of the source is not symmetrical or antisymmetrical with respect to $y = 0$ (either skew source field distribution or the source placed outside $y = 0$), the source field must be analyzed in symmetrical plus antisymmetrical modes of the duct section where the source is placed; the above analysis must then be performed for both types of symmetry, and the fields for them finally superimposed. Because the duct modes are orthgonal, the modal analysis of the source field is performed by standard techniques. The duct section containing the source plays the role of the entrance duct in the above analysis; the duct mode components of the source field are the "incident modes" from above. If the lateral walls of the wedge are also inclined (producing a conical duct), the analysis is principally the same; but the formulation and the numerical computation blows up from a two-dimensional modal analysis to a three-dimensional analysis.

As was indicated in the introduction, the immense literature about underwater sound fields in wedge-shaped spaces with an absorbing boundary cannot be applied for the present task because of the severe restriction to very small wedge angles of the underwater acoustic theoretical approximations. It should, however, not be overlooked that the present method of stepped duct sections as an

approximation to a wedge also has an inherent upper limit of the wedge angle ($\alpha \approx 50^\circ$). Larger angles would need larger numbers I of sections, and the numerical errors of the modal analysis would increase. A succeeding paper will treat the case of wedge angles π and 2π by a different method; such wedge angles appear in the analysis of screens which are sound absorbing on one or both sides.

REFERENCES

1. F. P. MECHEL 1998 *Journal of Sound and Vibration* **216**, 649–671. Modes in lined wedge-shaped ducts.
2. F. P. MECHEL 1998 *Schallabsorber*, *Vol. III*, *Anwendungen*. Stuttgart: S. Herzel Verlag. See chapter 33 "Kanal mit Sprung" and chapter 34 "Daempferstrecke und Daempferkaskade".
3. J. M. ARNOLD and L. B. FELSEN 1984 *Journal of the Acoustical Society of America* **76**, 850–860. Intrinsic modes in a nonseparable ocean waveguide.
4. E. TOPUZ and L. B. FELSEN 1985 *Journal of the Acoustical Society of America* **78**, 1735–1745. Intrinsic modes: numerical implementation in a wedge-shaped ocean.